DISTRIBUTION OF THE H_2O MASERS IN THE SAGITTARIUS B2 CORE

H. Kobayashi[1], M. Ishiguro[1], Y. Chikada[1], N. Ukita[1],
K-I. Morita[1], S. Okumura-kawabe[1,2], T. Kasuga[1], and R. Kawabe[1]
1. Nobeyama Radio Observatory, Minamimaki-mura, Minamisaku-gun, Nagano 384-13
2. Department of Astronomy, Faculty of Science, University of Tokyo, Bunkyo-ku, Tokyo 113

ABSTRACT. The distribution of H_2O masers in the Sgr B2 core was observed with a 2.5'x2.5' wide field and with 540 km s^{-1} total velocity coverage by the Nobeyama Millimeter Array. Thirty-nine resolved maser spots were detected with a relative positional accuracy of 0.3", which are clustered into four separate regions. In Sgr B2 north, the cluster lies at the edge of the continuum ridge. One of the maser spots shows strong and wide velocity-spread emission, suggesting it may correspond to a center of star forming activity. In Sgr B2 main, the strong maser spots are projected just on the face of a compact HII region, and are red-shifted relative to the central velocity of the HII region. There are two possibilities to interpret our results in Sgr B2 (M). One is that the H_2O maser spots are distributed around the HII region and are infalling to the HII region. The other is that the H_2O maser sources are associated with the cloud in the foreground of the HII region.

1. Introduction

The Sgr B2 region is one of the most active star forming regions, lying about 200 pc from the Galactic Center. The core has a size of 5-10 pc, a mass of $\sim 10^5$ $M_\odot$, and a luminosity of $\sim 10^6$ $L_\odot$ (Erickson et al. 1977; Gatley et al. 1978). The presence of H_2O masers is an indicator of active star formation. H_2O maser emission is thought to arise from compact ($\sim 10^{13}$ cm) and dense ($n(H_2) \sim 10^{9-11}$ cm^{-3}) clumps of gas (Downes 1985; Reid and Moran 1981). H_2O masers have become a good probe of active star formation. In order to investigate the physical conditions of the H_2O maser emitting regions and their association with continuum and other molecular line emission, high positional accuracy measurements are needed as well as wide velocity coverage of all spectral components. The Nobeyama Millimeter Array (Ishiguro, et al., 1984) is well suited to observe the whole maser distribution in the Sgr B2 core, with its large (5' x 5') field of view, and wide (544 km s^{-1}) velocity coverage.

2. Observations and Data Analysis

The observational parameters are summarized in Table 1. Figure 1 shows the uv-coverage of our observations. The visibilities of the

M. Morris (ed.), The Center of the Galaxy, 181–187.

continuum emission were estimated from channels without maser emission. They were subtracted from all channels.

Table 1. Observation Parameters

Source	Sagittarius B2
Field Center	$\alpha(1950) = 17^h44^m10.4^s$
	$\delta(1950) = -28°22'00.0"$
Date of observation	1985.12.19
Baseline	Maximum Minimum
	540 (m) 60 (m)
Synthesized beam	4"x14"(αxδ)
Visibility calibrator	NRAO530 (7.2 Jy)
Bandpass calibrator	3C84
Rest frequency	22235.1 MHz
Total bandwidth	40 MHz (544 km s^{-1})
Velocity resolution	0.5 km s^{-1} (39 KHz)

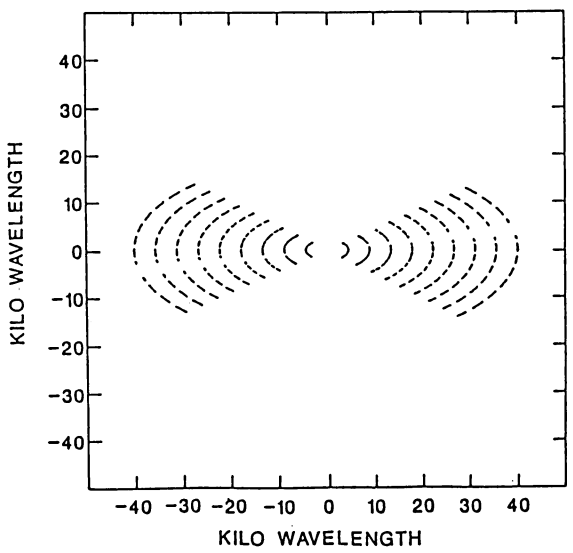

Figure 1. The uv-coverage of our observation. The synthesized beam size is 4"x14".

We used the self-calibration technique (Schwab, 1980) to suppress the effects of complex antenna gain errors and determine the precise relative positions of the H_2O maser spots. First, we selected a strong (576 Jy), isolated maser component at 29.5 km s^{-1} for a self-calibration model of a single point source. We solved for the complex antenna gains and applied them to other channels to minimize the phase and amplitude errors.

The positional accuracy of this reference component was determined by visibility calibration errors, phase fluctuation, baseline errors and differential propagation delay due to the curvature of the atmosphere. Two observations were carried out with different array configurations on Dec. 19, 1985 and Jun. 18, 1986. In these two observations, the profile of the H_2O maser emissions changed (Kobayashi et al. in preparation). The absolute positions of the maser clusters were found to repeat within 1"x3" (αxδ) between two independent observations.

After self-calibration and CLEANing (Högbom 1974), the dynamic range of the map for the reference component was estimated to be about 100:1 (peak to rms). The noise of channel maps without maser emissions is 0.2 Jy/beam rms. The relative positional accuracy of maser components, whose flux density is above 9 Jy, is limited by the cell size (0.3" x 0.3") and the dynamic range of maps (Thompson, Moran, and Swenson, 1986). For

https://doi.org/10.1017/S0074180900186516 Published online by Cambridge University Press

weaker components, the relative positional accuracy is limited by the system noise.

3. Results & Discussion

Figure 2 shows the spectrum of the H_2O maser emission integrated over the 2.5' x 2.5' field centered on Sgr B2 (M). The velocity spread of the H_2O maser components extends from -26 km s^{-1} to 114 km s^{-1}. Strong maser features are shown from 30 km s^{-1} to 70 km s^{-1}, which are near the central velocity of HII regions. High velocity features are weaker than these low velocity features. Since the dynamic range is limited to 100:1, weaker features would be missed at low velocities.

Figure 3 shows the positions of the H_2O maser components, superimposed on a 5 GHz continuum map of the Sgr B2 region by Benson and Johnston (1984). We will follow the continuum source notations adopted by Benson and Johnston (1984). Maser spots, shown as dots on the diagram, form four distinct clusters; in each of them an H_2CO maser has been found by Gardner et al. (1986). We have found a new H_2O maser cluster lying between Sgr B2 (N) and Sgr B2 (M). In the vicinity of this cluster, OH and H_2CO masers have also been detected (Benson and Johnston 1984; Garay et al. 1985; Gardner et al. 1986), but no continuum emission is observed.

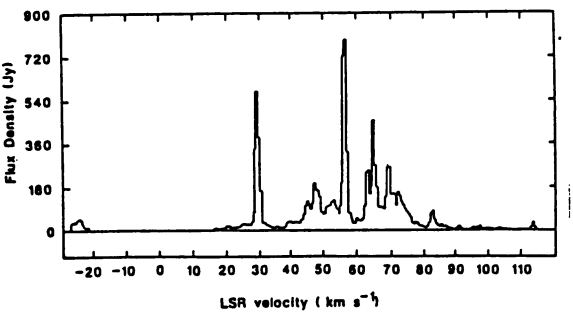

Figure 2. Spectra of H_2O maser emission extend from -26 km s^{-1} to 114 km s^{-1}. The -26 km s^{-1} component is isolated from the other maser emission components

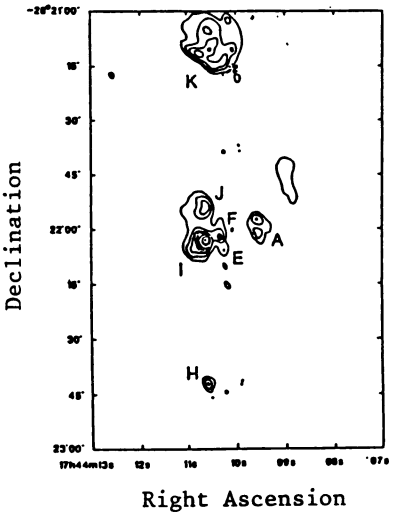

Figure 3. Distribution of H_2O maser spots. The contour map is the 5 GHz continuum map by Benson and Johnston (1984). Dots show the H_2O maser spots. Asterisks show H_2CO masers detected by Gardner et al. (1986).

In Sgr B2 (S), three H_2O maser spots were found. These are probably associated with the HII region H shown on figure 3 and OH and H_2CO maser sources.

https://doi.org/10.1017/S0074180900186516 Published online by Cambridge University Press

In two strong maser regions, Sgr B2 (M) and (N), the positions of maser spots are concentrated to 4" x 4" (0.2 pc x 0.2 pc) and 1" x 2" (0.05 pc x 0.1 pc) ($\alpha x \delta$), respectively. Dense regions are probably formed around the center of star forming activity in these small areas. In other maser sources, strong maser spots are also concentrated into areas of $\sim$0.1pc (Genzel et al. 1978). We will show results of these regions in detail.

a) Sgr B2 (N)

We have resolved the northern cluster into 15 individual maser spots spatially (labelled a to o in Fig. 4); and 23 spectral components were identified in Sgr B2 (N). Maser spots are located at the edge of the diffuse HII region K, and are spread over a 4" x 4" area. The spectrum of the H_2O maser emission from Sgr B2 (N) (Fig. 5) extends over a velocity range from 15 km s^{-1} to 115 km s^{-1}. The Sgr B2 (N) cluster has the most extended velocity range and the highest integrated intensity of the maser emission in the Sgr B2 core region. Half of the total maser power emitted from Sgr B2 (N) comes from spot j; its spectrum covers a velocity range from 20 km s^{-1} to 55 km s^{-1} (displayed by the shaded area in Fig. 5). Spot c in Fig. 4 has the highest peak flux density (576 Jy) in the Sgr B2 (N) cluster. The powers of the H_2O masers from spot j and c are 3.9×10^{-3} $L_\odot$ and 2.7×10^{-3} $L_\odot$, respectively. They are one order of magnitude higher than those for maser sources around Orion KL IRc2.

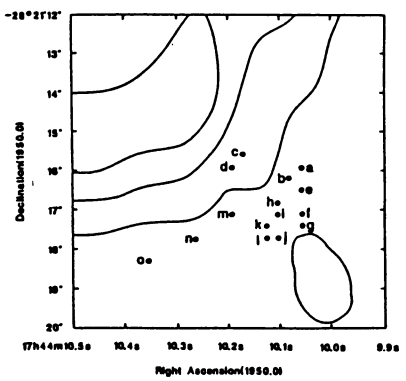

Figure 4. Detailed distribution of H_2O maser spots in the Sgr B2 (N). positions of the maser spots are indicated by dots, superimposed on a 5 GHz continuum map. The beam size is 2.7" x 1.6" at P.A.= 11°.7. The contour levels are at 29 x (2,3,4) mJy per beam.

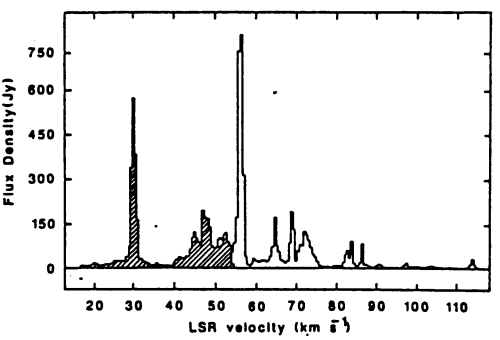

Figure 5. Spectrum of H_2O maser emission from Sgr B2 (N). The The shaded area shows the spectrum from spot j. The spot j is blue-shifted to other maser components

The maser sources in spots a, b, e, f, g, h, and i are red-shifted to the central velocity (65 km s^{-1}) of the NH_3 emission (Vogel, Genzel and

https://doi.org/10.1017/S0074180900186516 Published online by Cambridge University Press

Palmer 1987) and the HC_3N(v=1,J=12-11) emission (Goldsmith et al 1987). They exist in the same direction of the red-shifted molecular outflow observed by NH_3 emission. These maser sources are probably associated with the red-shifted component of the molecular outflow, similar to the high velocity maser sources around Orion KL IRc2 (Genzel et al. 1981a). The velocities of the maser components associated with spot j are blue-shifted.

b) Sgr B2 (M)

The Sgr B2 (M) cluster has been resolved into 7 individual spots spatially (Fig. 6); and 11 maser components are identified. The profile of Sgr B2 (M) is shown in Fig. 7. All of the spots, except v, are located close to the HII region F. The maser components are concentrated toward spots q and r, which have a velocity range extending from 35 km s^{-1} to 70 km s^{-1} (shown by the shaded area in Fig. 7). There are two extremely blue shifted spots u and v which lie spatially separated from spots p, q, r, s and t. Strong components (>30 Jy) are red-shifted relative to the central velocity (60.3 km s^{-1}) of the H76α recombination line. The positions of the H_2O maser spots from 35 km s^{-1} to 70 km s^{-1} coincide with the positions of the OH and H_2CO maser spots within the positional errors of each observations (Benson and Johnston 1984; Gardner et al., 1986).

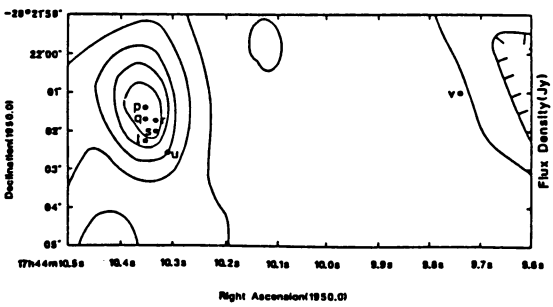

Figure 6. Detailed distribution of H_2O maser components in Sgr B2 (M), superimposed on the 5 GHz continuum map. The contour levels are at 29 x (2,3,4,5,6,7) mJy per beam. The beam size is 2.7" x 1.6" at P.A.= 11°.7. The positions of maser spots are indicated by the dots.

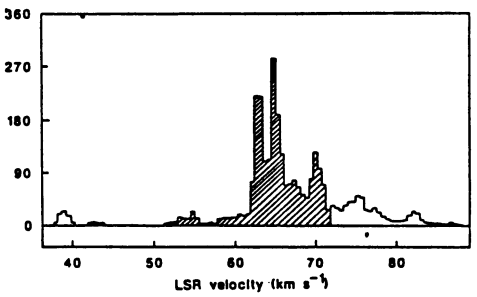

Figure 7. Spectrum of H_2O maser emission from Sgr B2 (M). The shaded area shows spectral components emitted from spots q and r.
The H_2O maser emission is concentrated into the velocity range from 60 km s^{-1} to 70 km s^{-1}.

The area covered by the ensemble of these maser spots is almost 1" x 1" and 0.04 pc x 0.04 pc at the Sgr B2 distance. This size agrees with the

https://doi.org/10.1017/S0074180900186516 Published online by Cambridge University Press

VLBI observations by Elmegreen et al. (1980). Since H_2O maser sources are compact (10^{13-14} cm) and dense (10^{10} cm^{-3}) (Downes, 1985), the velocities of H_2O maser sources are thought to trace the velocities of the compact area in the dense cloud core.

We can make two interpretations of our results, including molecular line and continuum observations. One is that the maser sources are associated with the HII region F and infalling onto it. Although the previous observations in the active H_2O maser region show the outflow of the H_2O maser spots, the infalling maser spots are suggested by the following observational information. 1) The H_2CO line emission has been observed by the absorption feature from 60 km s^{-1} to 75 km s^{-1} (Gardner et al., 1986). The strong H_2O maser spots, red-shifted to the central velocity (60 km s^{-1}) of the HII region F, are probably associated with this H_2CO cloud in the foreground of the HII region F. 2) The emission measure of the HII region F is 2.6×10^{9} cm^{-6} pc (Benson and Johnston 1984). Assuming the electron temperature T_e is 10000 K (Roelfesma et al. 1987), the optical depth of the HII region F is almost 2.2 at 22 GHz. Assuming the strong red-shifted maser spots are in the foreground of the HII region F and the weak blue-shifted maser spots are in the background, the cluster of the H_2O maser sources has the same central velocity as the HII region F and the intrinsic intensity of maser sources are almost the same around 60 km s^{-1}. In previous observations with the single dish telescopes, the red-shifted maser sources are stronger than the blue-shifted ones (Genzel, Downes, and Bieging 1976;Genzel and Downes 1977). This feature doesn't exhibit time variation. Then the H_2O maser sources are infalling toward the compact HII region F at 0.04 pc from the central star. If the H_2O maser sources and the H_2CO cloud are infalling to the HII region F at 10 km s^{-1}, the gravitational free fall mass is about 200 $M_\odot$. There is no model to explain the velocity width of the H_2O maser emissions

Another interpretation is that the H_2O maser sources are associated with the interacting region of the 60 km s^{-1} cloud around the HII region F and the 67 km s^{-1} cloud around the HII region E, which is observed by the meta-thermal OH lines (Gardner, Whiteoak, and Palmer, 1987). Since the 50 km s^{-1} and 70 km s^{-1} NH_3 and H_2CO clouds are observed by absorption lines (Vogel, Genzel, and Palmer 1987; Gardner et al., 1986), they exist in the foreground of the HII region F. By the observations of the OH meta-stable line emission, the peaks of molecular line emission are projected on the HII regions F and E with 60 km s^{-1} and 67 km s^{-1}, respectively. Since the H_2O maser emission is strong between 60 km s^{-1} and 70 km s^{-1}, it can be thought that the H_2O masers are pumped in the region of interaction between the 60 km s^{-1} cloud and the 67 km s^{-1} cloud. If the H_2O maser sources are associated with the interacting region of two molecular clouds, it is difficult to explain the coincidence that the area of maser emitting region is small and the H_2O, OH, and H_2CO masers are located just on the face of the HII region F.

References

Benson, J.M., and Johnston, K.J. 1984, Astrophys. J.,, 277 181
Downes, D. 1985, 'H_2O masers in Star-forming Regions', Birth and Infacy of Stars, Les Houches 1983, eds. R. Lucas and A. Omont
Elmegreen, B.G. et al., 1980, Astrophys. J., 241, 1007
Forster, J.R., et al., 1978, Astrophys. J., 221, 137
Garay, G., Reid, M.J., and Moran, J.M., 1985, Astrophys. J., 289, 681
Gardner, F.F. et al., 1986, M.N.R.A.S., 218, 385
Gardner, F.F., Whiteoak, J.B., and Palmer, P., 1987, M.N.R.A.S., 225, 467
Genzel, R., Downes, D., and Bieging, J., 1976, M.N.R.A.S., 177, 101p
Genzel, R., and Downes, D., 1977, Astron. Astrophys. Suppl., 30, 145
Genzel, R., et al., 1978, Astron. Astrophys. 66, 13
Genzel, R., et al., 1981a, Astrophy. J., 244, 884
Genzel, R., et al., 1981b, Astrophys. J., 247, 1039
Goldsmith, P.F., Snell, R.L., and Lis, D.C., 1987 Astrophys. J., 313, L5
Goldsmith, P.F. et al., 1987 Astrophys. J., 314. 525
Högbom, J.A., 1974, Astron. Astrophys. Suppl. 15, 417
Ishiguro, M., et al., 1984, Proceedings of the International Symposium on Millimeter and Submillimeter Wave Radio Astronomy, Granada
Kobayashi, H. et al., 1988, in preparation
Morris, M., 1976, Astrophys. J., 210, 100
Reid, M.J. and Moran, J.M., 1981, Ann. Rev. Astron. Astrophys., 19, 231
Roelfsema, P.R., et al., 1987, Astron. Astrophys., 175, 219
Schneps, M.H., 1981, Astrophys. J., 249, 124
Schwab, F., 1980, Proc. Soc. Photo-Opt. Instr. Eng., 231, 18
Thompson, A.R., Moran, J.M., and Swenson, G.W., 1986, Interferometry and Aperture Synthesis in Radio Astronomy, 411-417, John Wiley & Sons
Vogel, S.N., Genzel, R., and Palmer, P., 1987 Astrophys. J. 316, 243